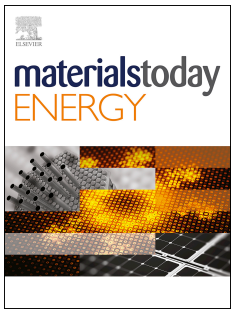

Turbine Disk-Type Triboelectric Nanogenerator for Wind Energy Harvesting and Self-Powered Wild Fire Pre-Warning

Xiaobo Gao, Fangjing Xing, Feng Guo, Yuhan Yang, Yutao Hao, Jun Chen, Baodong Chen, Zhong Lin Wang

PII: S2468-6069(21)00232-X

DOI: https://doi.org/10.1016/j.mtener.2021.100867

Reference: MTENER 100867

To appear in: *Materials Today Energy*

Received Date: 30 July 2021

Revised Date: 23 September 2021

Accepted Date: 24 September 2021

Please cite this article as: X. Gao, F. Xing, F. Guo, Y. Yang, Y. Hao, J. Chen, B. Chen, Z.L. Wang, Turbine Disk-Type Triboelectric Nanogenerator for Wind Energy Harvesting and Self-Powered Wild Fire Pre-Warning, *Materials Today Energy*, https://doi.org/10.1016/j.mtener.2021.100867.

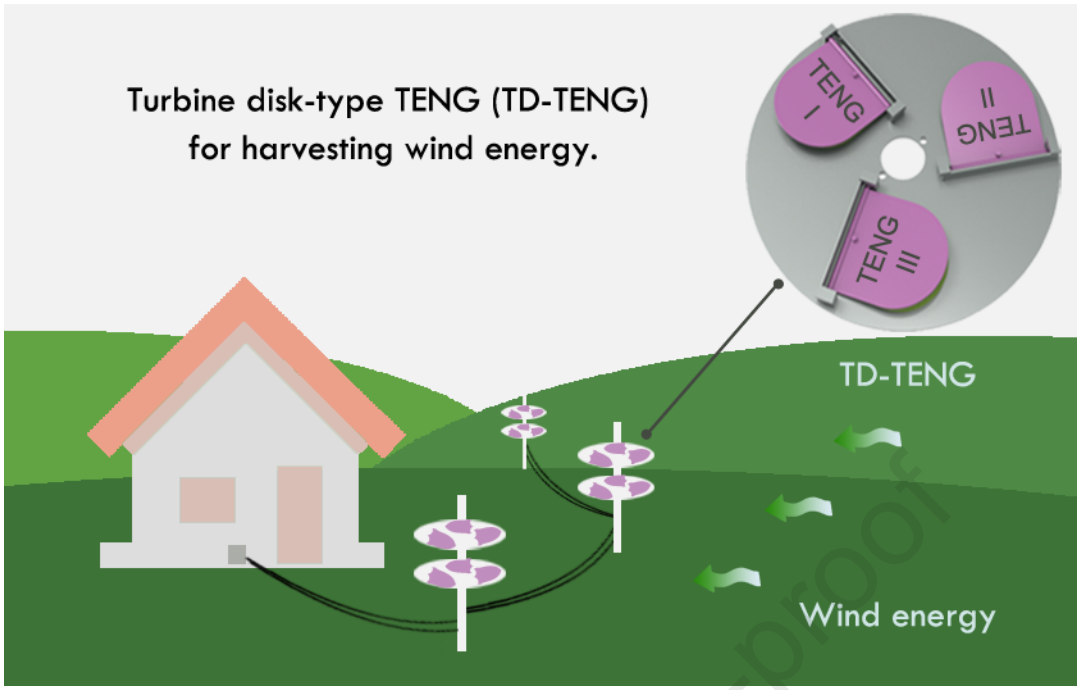

Article type: Full Paper

Turbine Disk-Type Triboelectric Nanogenerator for Wind Energy Harvesting and Self-Powered Wild Fire Pre-Warning

Xiaobo Gao [a, b, #], *Fangjing Xing* [a, b, #], *Feng Guo* [b, *], *Yuhan Yang* [a, b], *Yutao Hao* [a, b], *Jun Chen*[e], *Baodong Chen* [a, c, d, *] *and Zhong Lin Wang* [a, c, f, g, *]

[a] Beijing Institute of Nanoenergy and Nanosystems, Chinese Academy of Sciences, Beijing 101400, P. R. China

[b] School of Materials Science and Engineering, Inner Mongolia University of Technology, Hohhot, 010051, P. R. China

[c] School of Nanoscience and Technology, University of Chinese Academy of Sciences, Beijing 100049, P. R. China

[d] Institute of Applied Nanotechnology, Jiaxing, Zhejiang, 314031, P. R. China

[e] Department of Bioengineering, University of California, Los Angeles, Los Angeles, CA, 90095, USA

[f] CUSTech Institute, Wenzhou, Zhejiang, 325024, P. R. China

[g] School of Materials Science and Engineering, Georgia Institute of Technology, Atlanta, GA 30332-0245, USA

[#] X. G., and F. X., these authors contributed equally to this work.

* Co-corresponding authors: F. G., B. C., and Z.L. W.

E-mail: guofengnmg@sina.com; chenbaodong@binn.cas.cn; zlwang@gatech.edu

Abstract

We report a new type of turbine disk-type triboelectric nanogenerator (TD-TENG) to effectively convert small-scale wind energy into electricity. A unique double-floor TENG has been designed and its configuration has been carefully optimized by applying different polymer layers, contact areas and opening angles. With an optimized contact area of 83 cm^2, the TD-TENG delivers an open-circuit voltage of 230 V, a short-circuit current of 9 μA, and a peak power of 0.37 mW under an external load of 7 MΩ. Based on the TD-TENG, a self-powered wild fire pre-warning system has been constructed for temperature and fire monitoring. Such new TD-TENGs represent a promising sustainable energy solution for the distributed electronics in the era of Internet of things.

Keywords: Triboelectric nanogenerator, wind energy harvesting, turbine disk-type, self-powered sensing, pre-warning system

1. Introduction

5G and Internet of things (IoTs) have been significnatly changing our lives. Powering the distributed electron devices and sensor network sustainably is highly desired and remains a challenge [1-4]. Traditional fossil fuels are not only polluting the environment, but are also non-renewable and unaccommodated. So researchers have to explore new ways for supplying power [5-7]. Wind energy is renewable but remains underexplored due to the need for expensive equipment and high maintenance cost [8-11].

Invented in 2012, the triboelectric nanogenerator (TENG, also called as Wang generator) is a promising technology for converting mechanical energy into electricity [12,13]. It is based on the coupling effect of triboelectrification and electrostatic induction [14-16]. It is derived from the Maxwell's displacement current [17-21] which can effectively harness environmental mechanical energy sources such as wind [22-28], vibration [29,30], raindrop [31, 32], biomechanical [33-36], and blue energy [37-39]. Compared with traditional electromagnetic generators, Teng has unique advantages such as lightweight, facile manufacturing, high conversion efficiency, diverse selections of materials, and wide application range [40-42]. With the rapid development of IoTs over the last few decades, a large number of networked sensors are needed to collect and monitor big data. After entering the distributed age, the power supply should also be reformed accordingly. However, traditional power supply methods such as the cable transmission and the battery power supply, are costly and have difficulties in supplying power to sensors that are widely and remotedly distributed [43,44]. Therefore, it is necessary to build a sensor network where wireless transmission shall be one of the main transmission methods. Recently, on the basis of TENG, some researchers successfully demontrated self-powered portable electronic equipment and the liquid-surface fluctuation sensor to realize wireless transmission of alarm signals over a long distance [35,45]. At present, TENG is used to convert all kinds of mechanical energy into electricity to replace traditional electromagnetic

generators for distributed and sustainable power supply [46-49]. However, in most cases, the output performance of TENG degrades gradually due to the wear abrasion of triboelectric materials under long-term working conditions.

In this article, we present a new type of turbine disk-type TENG (TD-TENG) for harvesting wind energy. Our design is more suitable for operating conditions with low wind speed near the ground, and the system can be installed anywhere without impacting the environment. The turbine disk-type rotational structure can effectively avoid the wear between triboelectric materials even under the high rotational speed, showing overwhelming durability compared with the rotating-structured TENG. With a contact area of 83 cm^2, the TD-TENG delivers an open-circuit voltage of 230 V, a short-circuit current of 9 μA, and the peak power of 0.37 mW with an external load of 7 MΩ. Furthermore, relying only on the TD-TENG as a sustainable power source, a wireless self-powered wild fire pre-warning system has been successfully developed by the combination of the TD-TENG, a rectification circuit, a matching capacitor, an electronic thermometer, a signal transmitter, and a receiver. This combination improved the easiness and simpleness of the wild temperature and fire monitoring. This work greatly extends the applicability of TENG as an energy harvester and power source for distributed electronics.

2. Results and discussions

2. 1 Working principle of the TD-TENG

First, the double-floor TD-TENG has been carefully designed for wind energy harvesting (see Fig. 1). The double-floor TD-TENG device is fixed on a steel tube by conductive slip rings (Fig. 1b). The first floor and the second floor are provided with three pairs of the contact-separation TENG units. The diameter of the first floor and the second floor is 32 and 26 cm, respectively. Accordingly, the effective contact areas of the single fan blade are 83 and 44 cm^2, respectively. Figure 1c-e show the exploded view and materials of the contact-separation TENG unit used to manufacture the TD-TENG device. Thin aluminum (Al) electrodes are pasted on

the fan blade at the top and on the substrate at the bottom to collect the induced charge on the two triboelectric materials. The triboelectric layers containing fluorinated ethylene (FEP), polyimide (Kapton), Nylon, and polytetrafluoroethylene (PTFE) are pasted on the surface of the Al electrode at the top to be used for the comparative study of the output performance. The polypropylene (PP) film of the counter triboelectric layer is pasted on the surface of the Al electrode at the bottom. The detailed fabrication processes of the unit can be found in Experimental method. The TENG unit can work under both downwind and headwind conditions (see schematics in Fig. 1f). When the wind blows (downwind), the fan blade will be blew up to open up a certain angle to drive the turbine disk. Next, the turbine disk rotates to the point where the other fan blade is opened. The fan blade returns to its original state due to the effect of wind resistance. In this way, the three fan blades are lifted successively by the wind, and the turbine disk rotates clockwise around the steel pipe axis. The rising and falling processes correspond to the contact-separation working mode. The size of the pairs of fan blades on the turbine disk changes because of the different diameters of the first-floor and second-floor disks. The size of the fan blade has a direct effect on the working efficiency of the TD-TENG. When the fan blade area is enlarged, its mass increases so the required wind speed also becomes larger. Usually, the second-floor TD-TENG rotates faster than the first one when the wind speed is constant. Video S1 (Supporting Information) shows the working conditions under three different wind speeds.

The working mechanism of the TD-TENG is elaborated as follows (see schematics in Fig. 2a). In the initial state (Fig. 2a-I), when the triboelectric layer FEP film on the fan blade is in contact with the PP film on the base, the FEP film is negatively charged while the PP film has the same amount of positive charges. When the fan blade is lifted by the wind for a moment (Fig. 2a-II), the FEP film is more electronegative than the PP film due to the contact electrification. So, the FEP film tends to gain electrons to maintain an equal amount of positive charge on the bottom electrode. Then the charge is transferred from the upper electrode to the

lower electrode through an external circuit to maintain the balance of the electrostatic voltage. When the fan blade is completely lifted (Fig. 2a-III), the positive and negative charges of the upper and lower electrodes are equal, and there will be no charge transfer in the external circuit. When the fan blade rotates to the headwind state, the fan blade falls rapidly (Fig. 2a-IV). At this time, more electrons are acquired by the lower electrode. To maintain the electrostatic voltage balance, electrons are transferred to the upper electrode through the external circuit. As the rising and falling processes of the fan blade repeat regularly, the charge transfer induced by the upper and lower electrodes are also periodic. Therefore, the generator outputs AC signal. As shown in Fig. 2b, the finite element simulation results of the potential distribution (COMSOL software) verifies the feasibility of the TD-TENG.

2.2 Electrical output performance of the TD-TENG

To investigate the output performance quantitatively, a linear motor was used to precisely control the fan blade. The simulated blades were lifted by the wind and then returned to their original state by gravity and headwind. In this experiment, four different kinds of triboelectric materials such as FEP, Kapton, Nylon, and PTFE were selected to operate at a frequency of 1.5 Hz and with a fan blade area of 44 cm^2. The output power from the TD-TENG was gradually increasing in the order of PTFE, Kapton, Nylon, and FEP as shown in Fig. 3a-c. The transferred charge reached the maximum value of 50 nC under the short-circuit condition. The short-circuit current and the open-circuit voltage of the TD-TENG reached up to nearly 7 μA and 150 V, respectively. Therefore, the FEP and PP films were selected as two triboelectric materials for the TD-TENG to ensure optimized output performance.

After determining the optimal triboelectric materials, the effect of the contact area of the fan blades has to be considered. In this experiment, three sizes of the contact area were selected (Fig. 3d-f). The electricity generation unit delivered an transferred charge (Q_{SC}) of 22 nC, an open-circuit voltage (V_{OC}) of 60 V, and a short-circuit current (I_{SC}) of 3 μA with an effective

contact area of 19 cm^2. When the effective contact area was increased to 83 cm^2, the I_{sc} value could reach 9 μA and the Q_{SC} value was larger than 82 nC. The V_{oc} value was stable and exceeded 230 V peak to peak. With an increase in the contact area of the fan blade, an increase in both the wind resistance and wind speed was required. Therefore, two fan blades with the areas of 83 cm^2 and 44 cm^2 were selected as the first-floor and second-floor structures for the TD-TENG. Here, the second-floor TD-TENG was under normal running when the wind speed was very low. However, the first floor and the second floor work in an orderly manner simultaneously when the wind speed is high. Also, the second-floor TD-TENG rotated faster than the first-floor TD-TENG under a certain wind speed. The output performance of TENG is affected by the interaction between two triboelectric layers. Therefore, in order to identify the possible effects of fan blade quality, the mass of the fan blade was changed to verify the characteristics of the output in the experiments. Here, 5 g and 10 g of the weights were added to the fan blades with an area of 44 cm^2 (Fig. 3g and h). In addition, the effect of mass on the output performance of the TD-TENG with a fan blade area of 83 cm^2 is shown in Figure S1 (Supporting Information**)**, which shows no notable effect on the output performance by increasing the mass of the fan blade. The amount of transferred charge was nearly 50 nC and the open-circuit voltage was about 150 V. This was because the contact effect was closed to the saturated state when the output performance reached the optimal range. To avoid the influence of environmental humidity on the output performance and ensure the accuracy of the whole experiment, the test was carried out in an acrylic sealing cover with a dehumidifying fan (see the test equipment in Fig. 3i and Video S2). For the purpose of cost savings, good efficiency, and reduction in the demand level of wind speed, the most optimized structure was selected in the following experiment.

The influence of the openning angle on the contact effect was studied to optimize the output performance. The stroke of the linear motor was used to adjust the open-angle of the fan blade in the experiments as shown in Fig. 4a and Fig. 4b. From the experimental data, it could be seen

that the open-angle had no direct relationship with the output performance. The amount of transferred charge was nearly 52 nC and the open-circuit voltage was about 155 V. The output performance of the TD-TENG with an 83 cm^2 area fan blade with different openning angles has been investigated (see Figure S2, Supporting Information). To make the TD-TENG work more smoothly and have better rotation, the open-angle was increased to improve the wind resistance. The open-angle of the fan blade was adjusted to 90°. Fig. 4c and 4d show the test results on the influence of the running frequency on the output performance. The running frequency could be adjusted by a linear motor to be set to 1 Hz, 1.5 Hz, and 2 Hz. The transferred charge was nearly 51 nC and the open-circuit voltage was about 152 V in one cycle. More data on the effect of frequency on the output performance of the 83 cm^2 fan blade is provided in Supporting Information (Figure S3). It can be seen that there is no significant influence on the open-circuit voltage by increasing the running frequency. However, there was an increase in the number of transferred charges in unit time which shortened the charging time of the capacitor. Fig. 4e shows that the voltage increases and current decreases with an increase in the load resistance (measured at a working frequency of 1 Hz). The peak power of the TD-TENG was up to 0.37 mW under a load resistance of 7 MΩ (Fig. 4f). And then one, two, and three TENG units were sequentially integrated on the second-floor turbine disk (see the output performances in Fig. 4g-i). Moreover, the output performances of the first floor shown in Figure S4, illustrates that the working frequency of the whole device increases with the number of TENG units. The highest electric output was obtained with three TENG units. In practical applications, the working frequency (or rotational speed) of TD-TENG could be increased with increasing the wind speed.

2.3 Self-powered wild fire pre-warning system

Figure 5a shows the potential scene of the self-powered temperature sensor and wild fire pre-warning system. This system was composed of a double floor TD-TENG, six rectifier bridges,

a capacitor of 220 μF, a digital thermometer, a matching set of wireless transmitters and receivers, a switch, and a breadboard. The self-powered system can be placed on the grassland, desert, or other non-residential areas. Also, the novel double-floor TD-TENG can simultaneously light up 180 series LEDs (Figure S7 and Video S3). It can work as a distributed power source to drive smoke and temperature sensors, when there is an occurrence of wild fire in the grassland. To avoid power loss, six TENG units were connected to each of the six rectifier bridges (electrical diagrams shown in Fig. 5b and S5). The photograph of the double-floor TD-TENG based on six TENG units (Fig. 5c) has been deployed for practical applications in the wild (Fig. 5d). We first test the performance of charging capacitors by the TD-TENG under the laboratory fan with different capacitance (Fig. 5e) and different wind speeds (Fig. 5f). When the wind speed is higher, the working frequency of the TD-TENG becomes high and the amount of transferred charge also increases for the same charging time. Therefore, the charging curve under higher frequency takes less time to reach 3 V. To evaluate the stability, the 44 cm^2 size TENG unit was continuously tested at a frequency of 1.5 Hz (Fig. 5g). After the 1400 cycles, the transferred charges of the first and the last 50 cycles were recorded. They kept a consistent level of nearly 50 nC. For a detailed comparison, the enlarged views of the output waveform at the first and the last 5s were also presented. The results confirmed that the performance did not degrade during the long working duration (Figure S6). Figure 5h shows the important components of the self-powered temperature sensing system. The double floor TD-TENGs was used for charging a capacitor of 220 μF when it achieves a defined charging voltage of 2 V, which is about ten minutes under laboratory conditions. Then, the electronic thermometer is powered to detect the laboratory temperature to be 24.9 □ (the self-powered process is shown in Video S4).

For proof-of-concept demonstration, the self-powered fire pre-warning system has been constructed (see photographs in Fig. 5i and the circuit diagram in Fig. 5j). A video of the working device is provided in Video S5. After the capacitor of 220 μF was charged from 0 V to

about 3 V in 35 min, the transmitter will be driven to send a signal to the receiver, which turned on the alarm to send out sound and light when the switch was closed. The system can respond instantly to trigger the buzzer to emit a buzzing alarm. In an outdoor windy environment, the charging voltage of the capacitor reached a gate voltage of 3V in a shorter period, then the system is started and enters a real-time monitoring state. It is expected that the warning time will be shortened with increasing wind speed, which justifies the application in wild fire pre-warning.

3. Conclusion

We have presented a new type of TD-TENG, which can be utilized as both wind energy harvester and sustainable power source. In order to improve the practical applicability, a double floor TD-TENG device is designed and systematically optimized for wear minimization under rotational conditions. Harvesting wind energy near the ground with overwhelming durability has been demonstrated. Specifically, it delivers an open-circuit voltage of 230 V and a short-circuit current of 9 μA, transferred charge of 82 nC under the effective contact area of 83 cm^2, and the maximum peak power of 0.37 mW under an external load of 7 MΩ. Furthermore, a self-powered wild fire pre-warning system has been successful constructed by the combination of TD-TENGs, rectification circuit, matching capacitor, electronic thermometer, and signal transmission and receiver. It proves that, with an appropriate rectification circuit, the TD-TENGs can not only harvest wind energy near the ground, but also work as a distributed source for low-power electronics. This work provides a proof-of-concept demonstration for TENG toward multifunction practical applications under outdoor condition.

4. Experimental method

First of all, the first-floor and second-floor disks made of resin with diameters of 26 cm and 32 cm, respectively, were manufactured by 3D printing. Each turbine disk was fixed on the

stainless-steel tube through the conductive slip ring to ensure that the wires of the TENG unit could not twist due to the rotation of the turbine disk. Then, three pairs of two kinds of TENG units with effective contact areas of 44 cm^2 and 83 cm^2, respectively, were manufactured by 3D printing. Finally, they were fixed to the corresponding disks. The Al electrode film with a thickness of 20 μm was pasted on the lower and upper parts of the fan blade and the base, respectively. The whole unit consisted of a triboelectric membrane, a resin shell, and aluminum electrodes. The material of the triboelectric films on the top was FEP with a thickness of 80 μm. They had a polygon shape with areas of 55 cm^2 and 95 cm^2, respectively. The material of the triboelectric films on the bottom was polypropylene (PP) with a thickness of 80 μm. They had a polygon shape with areas of 44 cm^2 and 83 cm^2, respectively.

The output performance of the TD-TENG device was accurately measured under the ideal triggering generated by a linear motor. The short-circuit current, the open-circuit voltage, the transferred charge of the TENG device, and the charging voltage of different capacitors were measured by a current preamplifier (Keithley 6514 System Electrometer). The display and storage of data were performed by installing the software LabVIEW on the computer.

Credit Author Statement

Xiaobo Gao: Methodology, Data curation, Investigation. **Fangjing Xing**: Investigation, Visualization, **Feng Guo**: Writing- Original draft preparation, Supervision. **Yuhan Yang**: Formal analysis. **Yutao Hao**: Resources. **Jun Chen**: Validation, Formal analysis. **Baodong Chen**: Writing- Reviewing and Editing, Supervision, Resources. **Zhong Lin Wang**: Conceptualization, Supervision, Writing - Review & Editing.

Declaration of competing interest

The authors declare that they have no known competing financial interests or personal relationships that could have appeared to influence the work reported in this paper.

Acknowledgments

X. G., and F. X., contributed equally to this work. The authors acknowledge the support from Beijing Natural Science Foundation (Grant No.2192062), supported by National Natural Science Foundation of China (Grant No.51502147, 51702018, and 11704032). The research was sponsored by the National Key R & D Project from Minister of Science and Technology (2016YFA0202704), and the Beijing Municipal Science and Technology Commission (Z181100003818016 and Y3993113DF).

Appendix A. Supplementary data

The following is the Supplementary data to this article:

Corresponding Authors

*F. G., B. C., and Z.L. W.

E-mail: guofengnmg@sina.com; chenbaodong@binn.cas.cn; zlwang@gatech.edu

ORCID

Baodong Chen: 0000-0002-4647-0089

Zhong Lin Wang: 0000-0002-5530-0380

Keywords: Triboelectric nanogenerator, wind energy harvesting, turbine disk-type, self-powered sensing, pre-warning system

References

[1] G. Chen, Y. Li, M. Bick, J. Chen, Smart textiles for electricity generation, Chem Rev. 8, (2020) 3668-3720, https://doi.org/10.1021/acs.chemrev.9b00821.

[2] Y. Zou, V. Raveendran, J. Chen, Wearable triboelectric nanogenerators for biomechanical energy harvesting, Nano Energy. 77 (2020) 105303, https://doi.org/10.1016/j.nanoen.2020.105303.

[3] J. Chen, Y. Huang, N. Zhang, H. Zou, R. Liu, C. Tao, X. Fan, Z. L. Wang, Micro-cable structured textile for simultaneously harvesting solar and mechanical energy, Nat. Energy

10 (2016), https://doi.org/10.1038/nenergy.2016.138.

[4] X. Zhao, H. Askari, J. Chen, Nanogenerators for smart cities in the era of 5G and Internet of Things, Joule 5 (2021) 1391-1431, https://doi.org/10.1016/j.joule.2021.03.013.

[5] Z. L. Wang, Entropy theory of distributed energy for internet of things, Nano Energy 58 (2019) 669-672, https://doi.org/10.1016/j.nanoen.2019.02.012.

[6] X. Wang, Y. Zhang, X. Zhang, Z. Huo, X. Li, M. Que, Z. Peng, H. Wang, C. Pan, A highly stretchable transparent self-powered triboelectric tactile sensor with metallized nanofibers for wearable electronics, Adv. Mater., 30 (12) (2018), 1706738, https://doi.org/10.1002/adma.201706738.

[7] B. Chen, W. Tang, Z. L. Wang, Advanced 3D printing-based triboelectric nanogenerator for mechanical energy harvesting and self-powered sensing, Materials Today, (2021) https://doi.org/10.1016/j.mattod.2021.05.017.

[8] Z. Zhou, S. Padgett, Z. Cai, G. Conta, Y. Wu, Q. He, S. Zhang, C. Sun, J. Liu, E. Fan, K. Meng, Z. Lin, C. Uy, J. Yang, J. Chen, Single-layered ultra-soft washable smart textiles for all-around ballistocardiograph, respiration, and posture monitoring during sleep, Biosens. Bioelectron. 155 (2020) 112064, https://doi.org/10.1016/j.bios.2020.112064.

[9] L. Jin, X. Xiao, W. Deng, A. Nashalian, D. He, V. Raveendran, C. Yan, H. Su, X. Chu, T. Yang, W. Li, W. Yang, J. Chen, Manipulating relative permittivity for high-performance wearable triboelectric nanogenerators, Nano Lett. 9 (2020) 6404-6411, https://doi.org/10.1021/acs.nanolett.0c01987.

[10] Y. Liu, B. Chen, W. Li, L. Zu, W. Tang, and Z. L. Wang, Bioinspired Triboelectric Soft Robot Driven by Mechanical Energy, Adv. Funct. Mater. (2021) 2104770, https://doi.org/10.1002/adfm.202104770.

[11] Z. Zhou, L. Weng, T. Tat, A. Libanori, Z. Lin, L. Ge, J. Yang, J. Chen, Smart insole for robust wearable biomechanical energy harvesting in harsh environments, ACS Nano 10 (2020) 14126-14133, https://doi.org/10.1021/acsnano.0c06949.

[12] F. R. Fan, Z. Q. Tian, Z. L. Wang, Flexible triboelectric generator, Nano Energy 2 (2012) 328-334, https://doi.org/https://doi.org/10.1016/j.nanoen.2012.01.004.

[13] G. Chen, Y. Li, M. Bick, J. Chen, Smart textiles for electricity generation, Chem. Rev. 120 (2020) 3668e3720, https://doi.org/10.1021/acs.chemrev.9b00821.

[14] Z. L. Wang, A. C. Wang, On the origin of contact-electrification, Mater. Today, 30 (2019) 34-51, https://doi.org/10.1016/j.mattod.2019.05.016.

[15] N. Luo, Y. Feng, L. Zhang, W. Sun, D. Wang, X. Sun, F. Zhou, W. Liu, Controlling the tribological behavior at the friction interface by regulating the triboelectrification, Nano

Energy, 87 (2021) 106183, https://doi.org/10.1016/j.nanoen.2021.106183.

[16] S. Pan, Z. Zhang, Fundamental theories and basic principles of triboelectric effect: A review, Friction 7 (2019) 2-17, https://doi.org/10.1007/s40544-018-0217-7.

[17] Z. L. Wang, On the first principle theory of nanogenerators from Maxwell's equations, Nano Energy 68 (2020)104272, https://doi.org/10.1016/j.nanoen.2019.104272.

[18] Z. L. Wang, On Maxwell's displacement current for energy and sensors: the origin of nanogenerators, Mater. Today 20 (2017) 74-82, https://doi.org/10.1016/j.mattod.2016.12.001.

[19] J. Shao, M. Willatzen, T. Jiang, W. Tang, X. Chen, J. Wang, Z. L. Wang, Quantifying the power output and structural figure-of-merits of triboelectric nanogenerators in a charging system starting from the Maxwell's displacement current, Nano Energy 59(2019) 380-389, https://doi.org/10.1016/j.nanoen.2019.02.051.

[20] J. Shao, M. Willatzen, Y. Shi, Z. L. Wang, 3D mathematical model of contact-separation and single-electrode mode triboelectric nanogenerators, Nano Energy, 60 (2019) 630-640, https://doi.org/10.1016/j.nanoen.2019.03.072.

[21] R.D.I.G. Dharmasena, K.D.G.I. Jayawardena, C.A. Mills, J.H.B. Deane, J.V. Anguita, R.A. Dorey, S.R.P. Silva, Triboelectric nanogenerators: providing a fundamental framework, Energy Environ. Sci. 10 (2017) 1801, https://doi.org/10.1039/C7EE01139C.

[22] D. Liu, B. Chen, J. An, C. Li, G. Liu, J. Shao, W. Tang, C. Zhang, Z. L. Wang, Wind-driven self-powered wireless environmental sensors for internet of things at long distance, Nano Energy 73 (2020) 104819, https://doi.org/10.1016/j.nanoen.2020.104819.

[23] M. Wu, Z. Gao, K. Yao, S. Hou, Y. Liu, D. Li, J. He, X. Huang, E. Song, J. Yu, X. Yu, Thin, soft, skin-integrated foam-based triboelectric nanogenerators for tactile sensing and energy harvesting, Mater. Today Energy 20 (2021) 100657, https://doi.org/10.1016/j.mtener.2021.100657.

[24] Y. Liu, J. Wen, B. Chen, M. Zheng, D. Liu, Y. Liu, W. Tang, J. Liu, D. Nan, Z. L. Wang, Electro-blown spinning driven by cylindrical rotating triboelectric nanogenerator and its applications for fabricating nanofibers, Applied Materials Today 19 (2020) 100631, https://doi.org/10.1016/j.nanoen.2018.10.075.

[25] M. Sakaguchi, M. Makino, T. Ohura, T. Iwata, Contact electrification of polymers due to electron transfer among mechano anions, mechano cations and mechano radicals, J. Electrost. (2014), https://doi.org/10.1016/j.elstat.2014.06.006.

[26] R.K. Pandey, H. Kakehashi, H. Nakanishi, S. Soh, Correlating material transfer and charge transfer in contact electrification, J. Phys. Chem. C (2018),

https://doi.org/10.1021/acs.jpcc.8b04357.

[27] D.J. Lacks, R. Mohan Sankaran, Contact electrification of insulating materials, J. Phys. Appl. Phys. (2011), https://doi.org/10.1088/00223727/44/45/453001.

[28] Y. Liu, G. Liu, T. Bu, C. Zhang, Effects of interfacial acid base on the performance of contact separation mode triboelectric nanogenerator, Mater. Today Energy 20(2021), https://doi.org/10.1016/j.mtener.2021.100686.

[29] C. Wu, H. Huang, S. Yang, G. Wen, Pagoda-shaped triboelectric nanogenerator with high reliability for harvesting vibration energy and measuring vibration frequency in downhole, IEEE Sens. J. 23 (2020) 13999-14006, https://doi.org/10.1109/jsen.2020.3007000.

[30] G. Khandelwal, A. Chandrasekhar, N.R. Alluri, V. Vivekananthan, N.P. Maria Joseph Raj, S.-J. Kim, Trash to energy: a facile, robust and cheap approach for mitigating environment pollutant using household triboelectric nanogenerator, Appl. Energy 219 (2018) 338e349, https://doi.org/10.1016/j.apenergy.2018.03.031.

[31] C. Yao, A. Hernandez, Y. Yu, Z. Cai, X. Wang, Triboelectric nanogenerators and power-boards from cellulose nanofibrils and recycled materials, Nano Mater. Energy 30 (2016) 103e108, https://doi.org/10.1016/j.nanoen.2016.09.036.

[32] M. Jošt, B. Lipovšek, B. Glažar, A. Al□Ashouri, K. Brecl, G. Matič, A. Magomedov, V. Getautis, M. Topič, S. Albrecht, Perovskite solar cells go outdoors: Field testing and temperature effects on energy yield, Adv. Energy Mater. 25 (2020) 2000454, https://doi.org/10.1002/aenm.202000454.

[33] S. Matsusaka, H. Maruyama, T. Matsuyama, M. Ghadiri, Triboelectric charging of powders: a review, Chem. Eng. Sci. 65 (22) (2010) 5781e5807, https://doi.org/10.1016/j.ces.2010.07.005.

[34] J. Wen, B. Chen, W. Tang, T. Jiang, L. Zhu, L. Xu, J. Chen, J. Shao, K. Han, W. Ma, Z. L. Wang, Harsh□Environmental□Resistant Triboelectric Nanogenerator and Its Applications in Autodrive Safety Warning, Adv. Energy Mater. (2018) 1801898, https://doi.org/10.1002/aenm.201801898.

[35] Y.-T. Jao, P.-K. Yang, C.-M. Chiu, Y.-J. Lin, S.-W. Chen, D. Choi, Z.-H. Lin, A textile-based triboelectric nanogenerator with humidity-resistant output characteristic and its applications in self-powered healthcare sensors, Nano Mater. Energy 50 (2018) 513e520.

[36] B. Chen, W. Tang, T. Jiang, L. Zhu, X. Chen, C. He, L. Xu, H. Guo, P. Lin, D. Li, J. Shao, Z. L. Wang, Three-dimensional ultra flexible triboelectric nanogenerator made by 3D printing, Nano Energy 45 (2018) 380-389, https://doi.org/10.1016/j.nanoen.2017.12.049.

[37] D. Jiang, B. Shi, H. Ouyang, Y. Fan, Z.L. Wang, Z.-M. Chen, Z. Li, A 25-year bibliometric

study of implantable energy harvesters and self-powered implantable medical electronics researches, Mater. Today Energy 16 (2020) 100386. https://doi.org/10.1016/j.mtener.2020.100386.

[38] Z. Li, Q. Zheng, Z.L. Wang, Z. Li, Nanogenerator-based self-powered sensors for wearable and implantable electronics, Research 2020 (2020) 8710686, https://doi.org/10.34133/2020/8710686.

[39] J. Zhao, D. Wang, F. Zhang, Y. Liu, B. Chen, Z. L. Wang, J. Pan, R. Larsson, Y. Shi, Real-Time and Online Lubricating Oil Condition Monitoring Enabled by Triboelectric Nanogenerator, ACS Nano. (2021), https://doi.org/10.1021/acsnano.1c02980.

[40] Z. Zhao, Y. Dai, S.X. Dou, J. Liang, Flexible nanogenerators for wearable electronic applications based on piezoelectric materials, Mater. Today Energy 20 (2021) 100690, https://doi.org/10.1016/j.mtener.2021.100690.

[41] M. Wang, N. Zhang, Y. Tang, H. Zhang, C. Ning, L. Tian, W. Li, J. Zhang, Y. Mao, E. Liang, Single-electrode triboelectric nanogenerators based on sponge-like porous PTFE thin films for mechanical energy harvesting and self-powered electronics, J. Mater. Chem. 5 (24) (2017) 12252e12257.

[42] M. Wu, K. Yao, D. Li, X. Huang, Y. Liu, L. Wang, E. Song, J. Yu, X. Yu, Self-powered skin electronics for energy harvesting and healthcare monitoring, Mater. Today Energy 21 (2021) 100786, https://doi.org/10.1016/j.mtener.2021.100786.

[43] K. Han, J. Luo, J. Chen, B. Chen, L. Xu, Y. Feng, W. Tang, Z. L. Wang, Self-powered ammonia synthesis under ambient conditions via N2 discharge driven by Tesla turbine triboelectric nanogenerators, Microsystems & Nanoengineering 7, 7 (2021), https://doi.org/10.1038/s41378-020-00235-w.

[44] R. Roman, J. Zhou, J. Lopez, On the features and challenges of security and privacy in distributed internet of things, Comput. Networks 10 (2013) 2266-2279, https://doi.org/10.1016/j.comnet.2012.12.018.

[45] B. Chen, W. Tang, C. He, C. R. Deng, L. J. Yang, L. P. Zhu, J. Chen, J. J. Shao, L. Liu, Z. L. Wang, Water wave energy harvesting and self-powered liquid-surface fluctuation sensing based on bionic-jellyfish triboelectric nanogenerator, Mater. Today 1 (2018) 88-97, https://doi.org/10.1016/j.mattod.2017.10.006.

[46] A. Chandrasekhar, V. Vivekananthan, G. Khandelwal, W.J. Kim, S.-J. Kim, Green energy from working surfaces: a contact electrification-enabled data theft protection and monitoring smart table, Mater. Today Energy 18 (2020) 100544, https://doi.org/10.1016/j.mtener.2020.100544.

[47] W. Ma, X. Li, H. Lu, M. Zhang, X. Yang, T. Zhang, L. Wu, G. Cao, W. Song, A flexible self-charged power panel for harvesting and storing solar and mechanical energy, Nano Energy 65 (2019) 104082, https://doi.org/10.1016/j.nanoen.2019.104082.

[48] M. Sahu, S. Hajra, J. Bijelic, D. Oh, I. Djerdj, H. J. Kim, Triple perovskite-based triboelectric nanogenerator: a facile method of energy harvesting and self-powered information generator, Mater. Today Energy 20 (2021) 100639, https://doi.org/10.1016/j.mtener.2021.100639.

[49] W. Ma, J. Zhu, Z. Wang, W. Song, G. Cao, Recent advances in preparation and application of laser-induced graphene in energy storage devices, Mater. Today Energy 18 (2020) 100569, https://doi.org/10.1016/j.mtener.2020.100569.

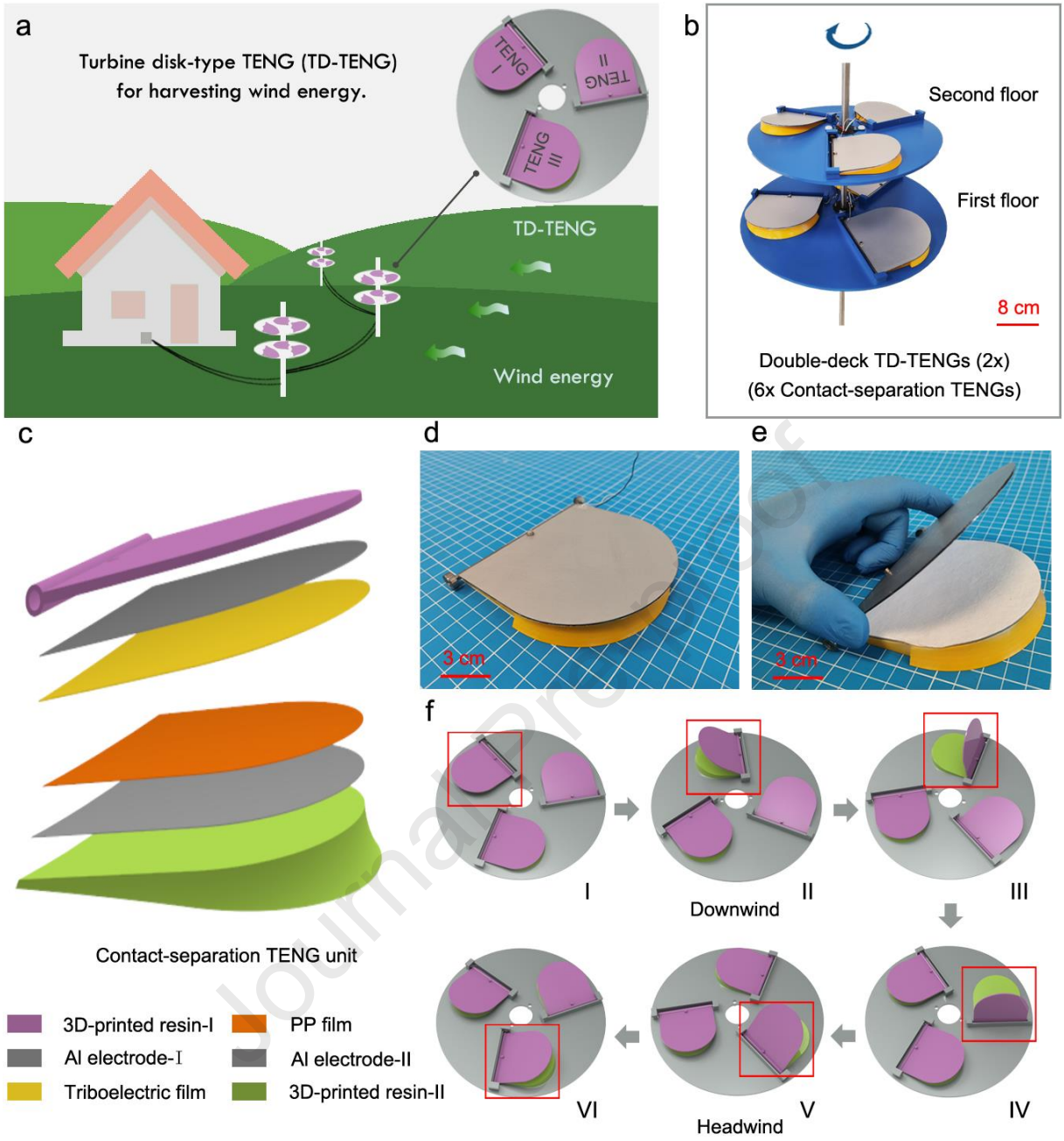

Fig. 1 Design and working process of the TD-TENG for wind energy harvesting. (a) Application scenario and overview of the TD-TENG for harvesting wind energy. (b) Schematic of the double-floor TD-TENG based on six TENG units. (c) Exploded view and corresponding materials of the TD-TENG. (d) and (e) Photographs of the TENG unit. (f) Working principle of the TD-TENG under the influence of wind.

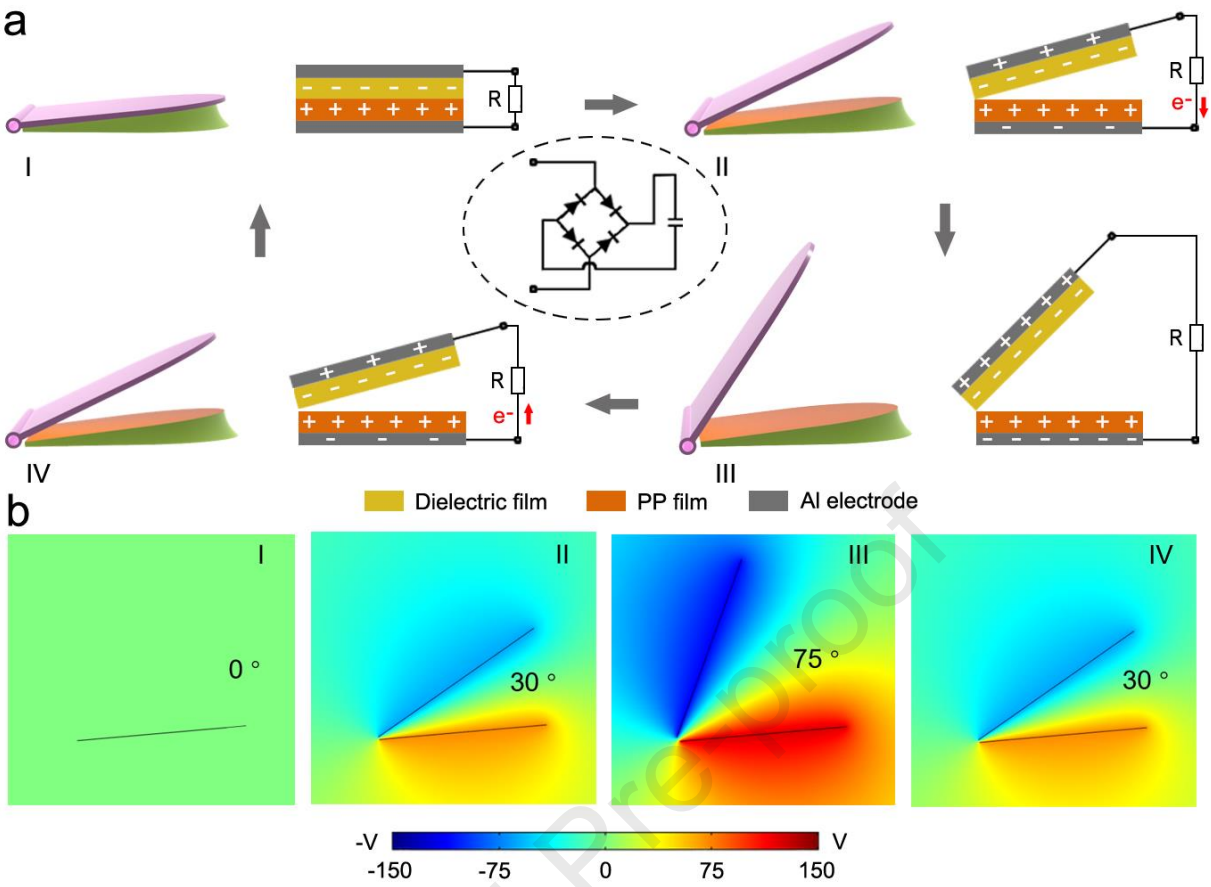

Fig. 2 Electricity generation and potential distributions. (a) Working mechanism of the TD-TENG under the four working states. (b) The finite element simulation results of the potential distributions under the four working states employing the COMSOL software.

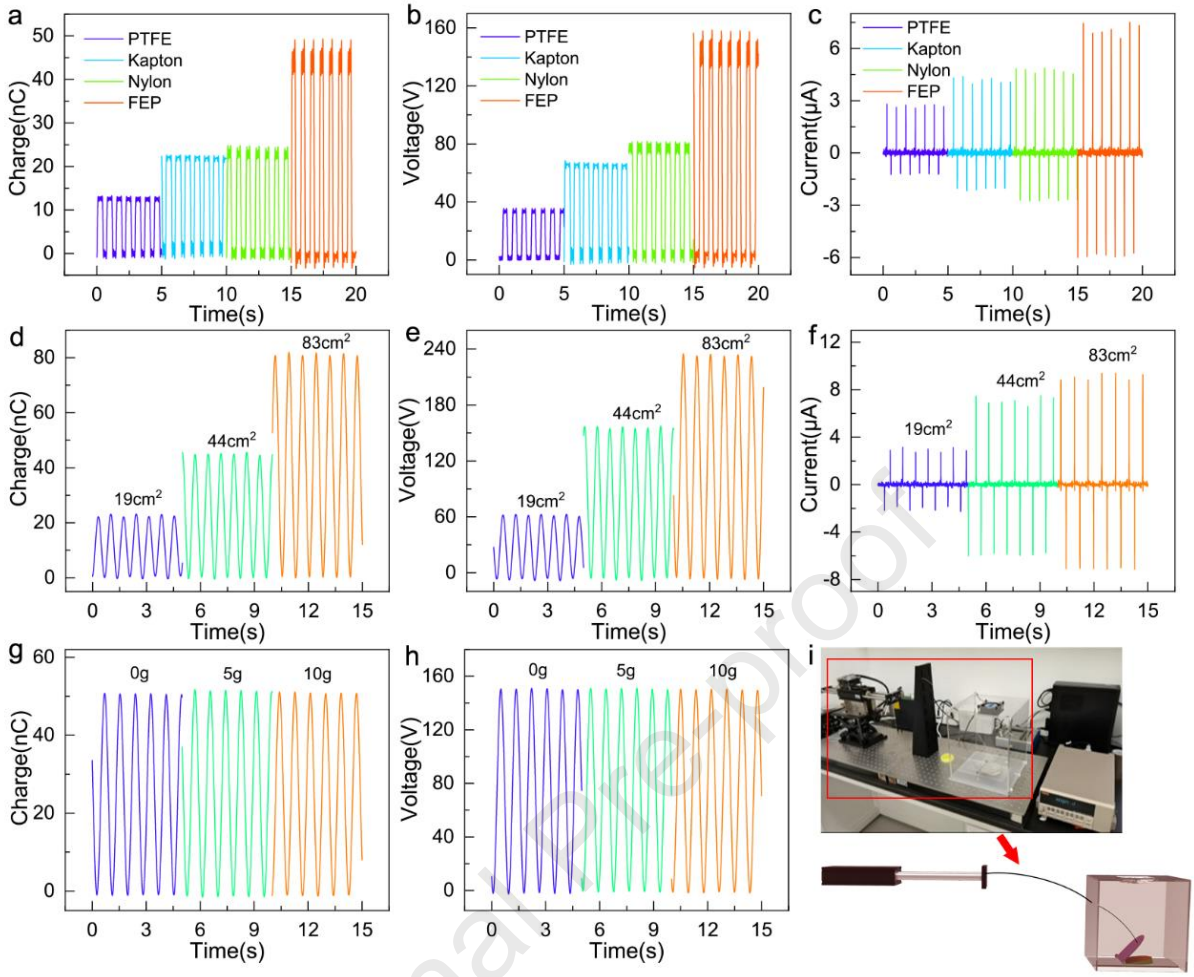

Fig. 3 Output performance of the TENG unit under different structural parameters. (a) Transferred charges, (b) open-circuit voltage, and (c) short-circuit current of the TENG unit with different triboelectric materials. (d) Transferred charges, (e) open-circuit voltage, and (f) short-circuit current of the TENG unit with different areas of the fan blade. (g) Transferred charges, and (h) open-circuit voltage of the TENG unit with different masses. (i) Photograph of the test equipment.

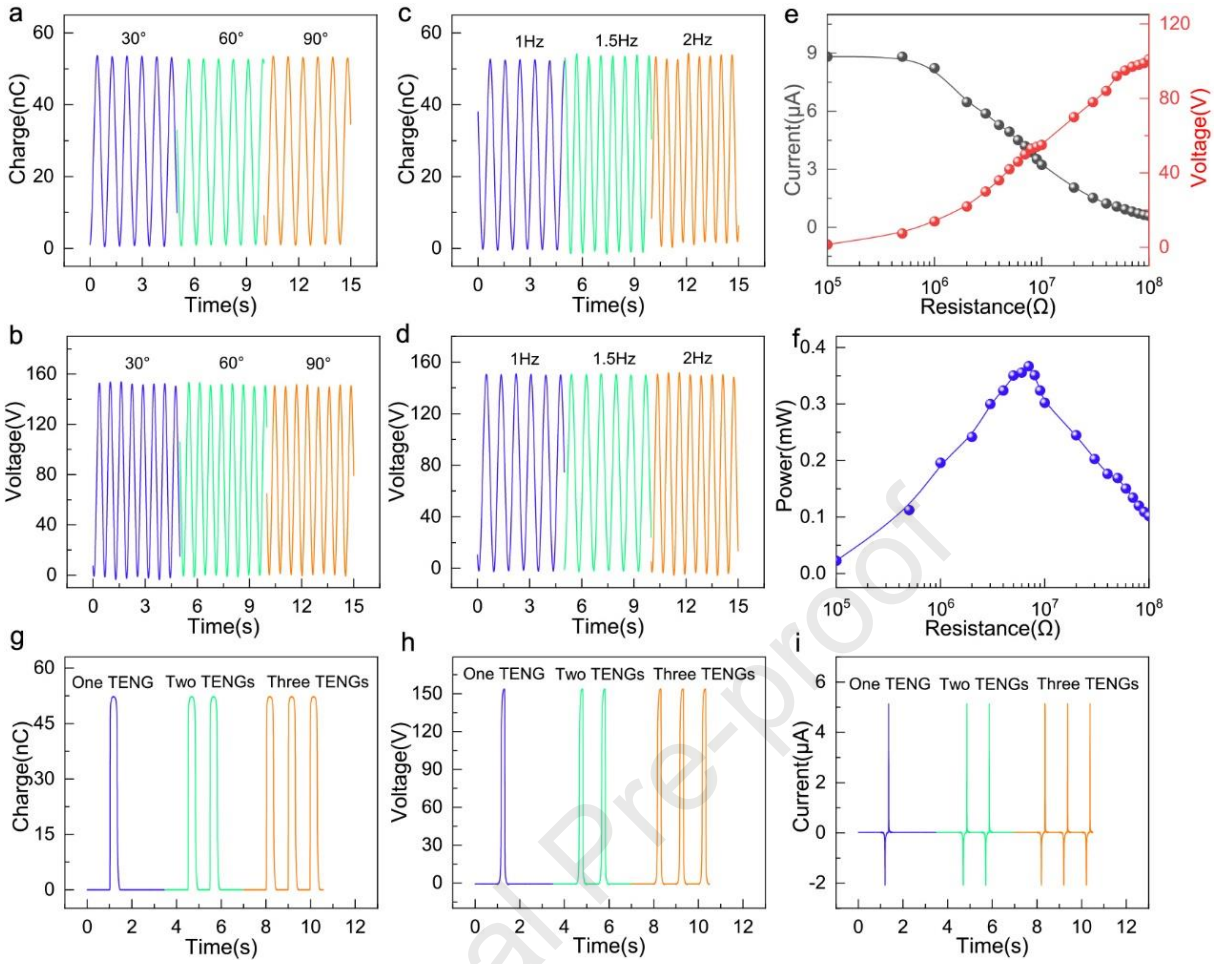

Fig. 4 Output performance of the TENG unit under different testing conditions. (a) Transferred charges, and (b) open-circuit voltage of the TENG unit at different open angles. (c) Transferred charges, and open-circuit voltage of the TENG unit at different working frequencies. (e) The voltage and current of the TENG unit under different load resistances. (f) Peak power of the TD-TENG. (g) Transferred charge, (h) open-circuit voltage, and (i) short-circuit current of the first-floor TD-TENG in one cycle.

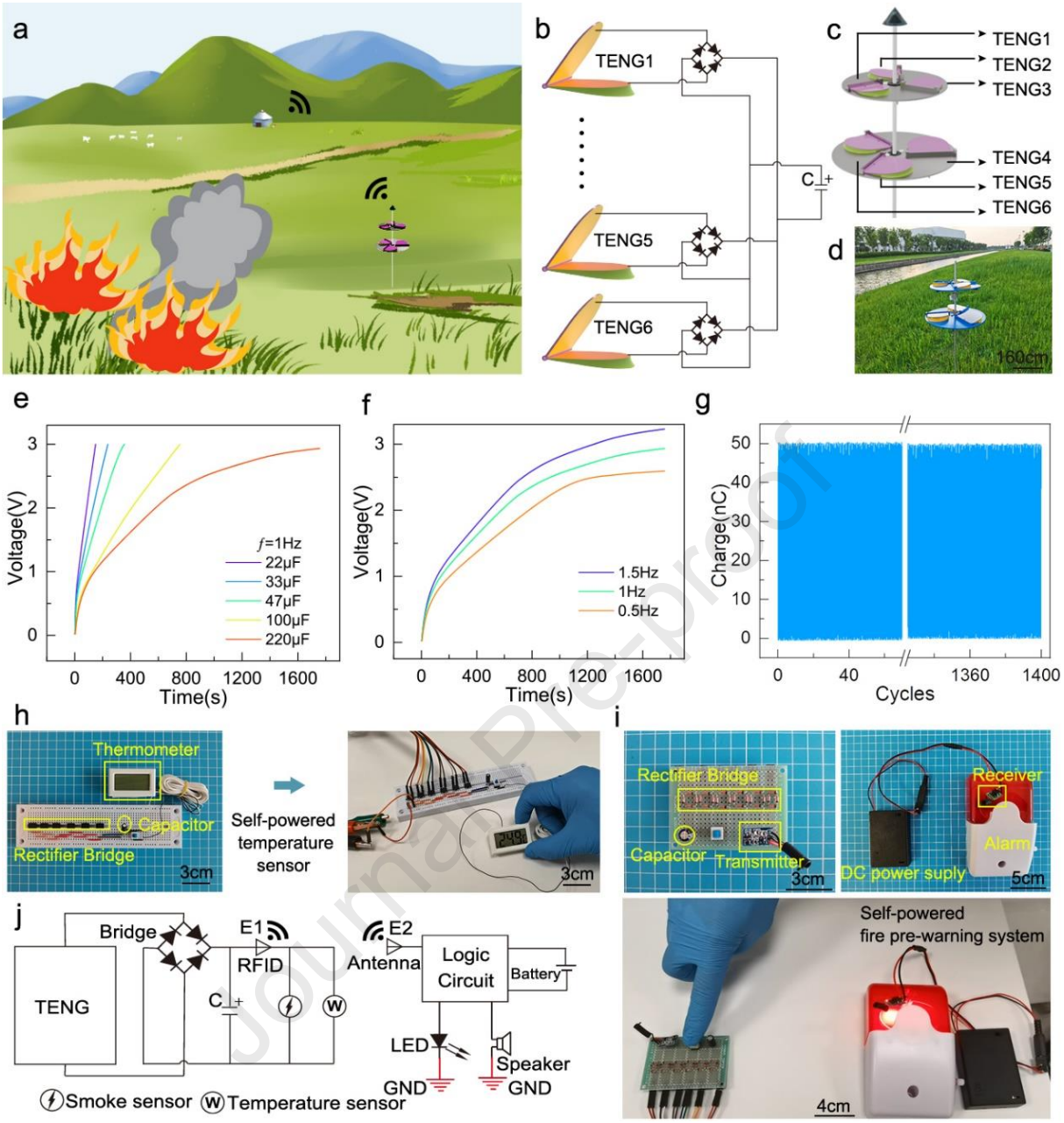

Fig. 5 Application of TD-TENG in wild fire pre-warning. (a) Application scene of the self-powered wild fire pre-warning system. (b) The circuit schematic diagram, (c) structure design, and (d) digital photograph of the system. (e) Charging curves of the double floor TD-TENGs for different capacitance under the working frequency of 1 Hz. (f) Voltage curves of a 220 μF capacitor charged under different working frequencies. (g) The output stability of the TD-TENG. (h) Photograph of the self-powered temperature sensing system. (i) Photograph of the self-powered wild fire pre-warning system. (j) The circuit principle of the self-powered system.

Highlights:

1. A unique design turbine disk-type triboelectric nanogenerator (TD-TENG) for harvesting wind energy near the ground.

2. Overwhelming durability and electrical output performances for harvesting breeze near the ground.

3. A distributed self-powered warning system has been demonstrated for prairies fire prevention.

Declaration of competing interest

The authors declare that they have no known competing financial interests or personal relationships that could have appeared to influence the work reported in this paper.

Credit Author Statement

Xiaobo Gao: Methodology, Data curation, Investigation. **Fangjing Xing**: Investigation, Visualization, **Feng Guo**: Writing- Original draft preparation, Supervision. **Yuhan Yang**: Formal analysis. **Yutao Hao**: Resources. **Jun Chen**: Validation, Formal analysis. **Baodong Chen**: Writing- Reviewing and Editing, Supervision, Resources. **Zhong Lin Wang**: Conceptualization, Supervision, Writing - Review & Editing.